Collaborative Control of Multivehicle Systems in Diverse Motion Patterns

Hai-Tao Zhang, Zhiyong Chen, and Ming-Can Fan

***Abstract*— In this brief, a decentralized control algorithm is proposed for a group of vehicles to form diverse collective motion patterns. Without the guidance of a global beacon or a global reference framework, the desired collective behavior occurs provided that the associated network of the multivehicle system is jointly connected. The effectiveness of the approach is verified through theoretical analysis, numerical simulation, and experimental results.**

***Index Terms*— Collaborative control, collective motion, multiagents, torus.**

I. Introduction

THE CHARACTERISTICS of a network of dynamic vehicles under collaborative control are exhibited by abundant sophisticated motion patterns. Typical motion patterns include migration (or flocking), swarming, and torus (see [1]–[3]). In particular, migration describes a multiagent system's assembled motion toward a common target with a fixed formation, swarming represents congregating motion in a bounded area, and torus means collective motion around a common center. The theoretical framework on collective behaviors of natural systems was also supported by the experimental results [4], [5].

Control engineers are interested in studying cooperative control strategies for autonomous multiagent systems to generate a certain collective motion pattern. For instance, torus behavior is a typical collective motion pattern, which has attracted considerable attentions of researchers over the past years. One of the earliest contributions on control of torus behavior was based on a virtual reference beacon model [6] that guides a group of vehicles to form circular motions. Later, in [7] and [8], more control algorithms were developed for collective stable circular motions with allowable equilibrium configurations. Circular motions were also studied in the scenario of cyclic pursuit in [9]–[11] when there is no virtual reference beacon. The cyclic pursuit formation is based on a fixed network topology, especially, represented by a circulant matrix. The result was further extended in [12] by introducing a more general rotation matrix for double-integrator dynamics. Along this research line, some recent works include [13] and [14] where some control protocols were proposed to make all agents surround a common point with a desired formation structure.

In [11]–[14], a technical feature is the analysis of the Laplacian corresponding to a fixed network topology, which requires the individuals to be labeled. For networks with time-varying network topologies, a framework on stabilization of planar collective motion was provided in [15]. This brief was based on identical steered particles moving in a plane with a uniform constant speed. It was further extended to 3-D space in [16]. The relevant problem was also studied in an alternative formulation of consensus on manifolds in [17]. A different control method was studied in [18], which guarantees global asymptotic stability of the circular motion. In such a configuration, however, a leader exists who always knows the position of the reference beacon.

More recently, a leader-free no-beacon algorithm was proposed for generating a collective circular motion behavior in [19] and [20]. It was shown that a stable torus phenomenon emerges under a certain jointly connected condition. The main technique used in [19] and [20] for each agent is to determine the center of its neighbor's circular motion based on velocity measurement and hence achieve consensus of motion centers. However, this idea cannot be extended to more complicated patterns. For example, it is impossible to determine the center of an elliptical motion based only on velocity measurement. One of the main contributions of this brief is to propose a new approach using the design of an additional reference model for each agent to investigate collective motions in more general patterns including circular motion as a special example. It is worth mentioning that the results in [19] and [20] are based on approximate stability analysis, but the new approach in this brief offers exact stability analysis.

With the reference models, the desired collective motion can be achieved through two concurrent actions, i.e., consensus of reference models and regulation of real vehicle trajectory to its associated reference model. In fact, such a two-step approach has been used for synchronization of heterogeneous multiagents, first for linear systems in [21] and [22]. More complicated situations were reported for nonlinear systems using feedforward design [23], internal model principle [24], and completely decentralized internal model principle [25], [26]. The main theoretical feature of this brief is that the two-step approach is used for the desired collective behavior when the associated network of the multiagent system is jointly connected, without the guidance of any global information such as a global beacon or a global reference framework.

Manuscript received February 5, 2015; revised June 9, 2015 and September 2, 2015; accepted September 26, 2015. Manuscript received in final form September 27, 2015. This work was supported in part by the National Natural Science Foundation of China under Grant 61322304, Grant 51328501, and Grant 51120155001, in part by the Australian Research Council under Grant DP130103039, and in part by the 973 Project under Grant 2015CB057304. Recommended by Associate Editor N. Olgac. *(Corresponding author: Zhiyong Chen.)*

H.-T. Zhang is with the Key Laboratory of Image Processing and Intelligent Control and the State Key Laboratory of Digital Manufacturing Equipment and Technology, School of Automation, Huazhong University of Science and Technology, Wuhan 430074, China (e-mail: zht@mail.hust.edu.cn).

Z. Chen is with the School of Electrical Engineering and Computer Science, The University of Newcastle, Callaghan, NSW 2308, Australia (e-mail: zhiyong.chen@newcastle.edu.au).

M.-C. Fan is with the Department of Mathematics, Huizhou University, Huizhou 516007, China (e-mail: mingcan.fan@gmail.com).

Color versions of one or more of the figures in this paper are available online at http://ieeexplore.ieee.org.

Digital Object Identifier 10.1109/TCST.2015.2487864

Also, it is for the first time that the proposed collective motion control method is verified by numerical simulation and experiments on a multiple-wheeled robot's platform.

The rest of this brief is organized as follows. In Section II, we introduce the dynamic vehicle model and formulate the problem of collaborative control of multiple vehicles in various patterns. The main control design approach is proposed in Section III. The numerical simulation and experimental results are discussed in Section IV. Finally, the conclusion is drawn in Section V.

II. Problem Formulation

We consider n vehicles moving in a plane equipped with a global reference framework Σ^g, which, however, is unknown to any vehicle. To better describe the group of vehicles, we denote the following two sets:

$$\mathbb{N} := \{1, \ldots, n\}, \quad \mathbb{E} := \{(i, j) | \, i, j \in \mathbb{N}, i \neq j\}. \tag{1}$$

For $i = 1, \ldots, n$, let $p_i \in \mathbb{R}^2$ and $u_i \in \mathbb{R}^2$ be the position and the velocity of vehicle i in its own coordinate framework Σ_i, which is different from Σ^g in general. The kinematic equation is given by

$$\dot{p}_i = u_i, \quad i = 1, \ldots n. \tag{2}$$

Suppose Σ^g is a reflection of Σ_i with a rotation $R_i \in \mathbb{R}^{2\times 2}$ and a translation $\xi_i \in \mathbb{R}^2$ where the rotation matrix is

$$R_i = \begin{bmatrix} \cos\rho_i & -\sin\rho_i \\ \sin\rho_i & \cos\rho_i \end{bmatrix}$$

for an angle $\rho_i \in \mathbb{R}$. Therefore, the position of vehicle i is, in the global reference Σ^g

$$p_i^g = R_i p_i + \xi_i.$$

Clearly, neither ρ_i (i.e., R_i) nor ξ_i is known to any vehicle.

We define a curve in the polar coordinates $(\wp(\theta), \theta)$ with the angular coordinate θ and the radial coordinate $\wp(\theta)$ by a continuously differentiable function $\wp(\theta) : \mathbb{R} \mapsto \mathbb{R}$ to describe a motion pattern. For example, $\wp(\theta) = 1, \forall\theta \in \mathbb{R}$ represents a circular motion pattern and

$$\wp(\theta) = \frac{ab}{\sqrt{(b\cos\theta)^2 + (a\sin\theta)^2}}, \quad a, b > 0 \quad \forall\theta \in \mathbb{R} \tag{3}$$

an elliptical motion pattern.

For a specified curve $\wp(\theta)$, the collective motion in the pattern $\wp(\theta)$ for a group of vehicles is defined as follows.

Definition 1: If there exist $q^o \in \mathbb{R}^2$ and $\sigma^o \in \mathbb{R}$, and time functions $\theta_i(t) : [0, \infty) \mapsto \mathbb{R}, i = 1, \ldots, n$, such that

$$\lim_{t\to\infty} p_i^g(t) - p_i^o(t) = 0, \quad i = 1, \ldots, n \tag{4}$$

for

$$p_i^o(t) := q^o + a_i\wp(\theta_i(t))\angle(\theta_i(t) + \sigma^o), \quad i = 1, \ldots, n \tag{5}$$

then the group of vehicles achieves the collective motion of the pattern $\wp(\theta)$. The notation $\angle\theta := [\cos\theta, \sin\theta]^\intercal$ is used in (5).

Remark 2: In the definition, q^o, σ^o, and a_i are the center, the orientation, and the size of the curve, respectively. As a_i represents the size of the curve, we can normalize $\wp(\theta)$ by assuming $\sup_{\theta\in\mathbb{R}}\wp(\theta) = 1$ without loss of generality. If $a_i = a_j, \forall i, j = 1, \ldots, n$, all vehicles share the pattern $\wp(\theta)$ of a unique size. The time function $\theta_i(t)$ determines the movement of vehicle i along the curve.

This brief aims to develop a decentralized controller for each vehicle to achieve the collective motion in the pattern $\wp(\theta)$. For the purpose of decentralized control, we define the neighborhood of each vehicle as follows, with the communication radius r:

$$\mathcal{N}_i(p^g) := \{j \in \mathbb{N} \mid \left\|p_i^g - p_j^g\right\| < r, \ j \neq i\}$$

for a complete position distribution $p^g := [(p_1^g)^\intercal, \ldots, (p_n^g)^\intercal]^\intercal$.

Suppose the controller is of the form

$$\begin{aligned} u_i &= k_i(z_i, p_i, \{\chi_{ij} \mid j \in \mathcal{N}_i(p^g)\}) \\ \dot{z}_i &= g_i(z_i, p_i, \{\chi_{ij} \mid j \in \mathcal{N}_i(p^g)\}). \end{aligned} \tag{6}$$

In the controller, p_i is the position (in the framework of Σ_i) of vehicle i and z_i is the state of the compensator. They are obviously available for vehicle i as control feedback. The measurement χ_{ij} is from the neighbor vehicle j, and more specifically

$$\begin{aligned} \chi_{ij} &= \{p_j, z_j, \ell_{ij}, \ell_{ji}\}, \ \ell_{ij} := R_i^{-1}\left(p_i^g - p_j^g\right) \\ \ell_{ji} &:= R_j^{-1}\left(p_j^g - p_i^g\right). \end{aligned}$$

In fact, ℓ_{ij} is the relative position between vehicles i and j, measured by vehicle i in the reference framework Σ_i, but p_j and z_j and ℓ_{ji} are transmitted to vehicle i from vehicle j. In general, $\ell_{ji} \neq -\ell_{ij}$ as they are measured in different reference frameworks.

In summary, the objective of this brief is to design a controller of the form (6) for each vehicle such that the group of vehicles achieves the collective motion of the pattern $\wp(\theta)$ in the sense of Definition 1. This control objective is sought in the scenario where the network satisfies a certain connectivity condition. More specifically, a so-called jointly connected condition is used in this brief. The definition given below is borrowed from [27].

Definition 3: Consider the group of vehicles (2).

- Let $\mathcal{E}(p^g) := \{(i, j) \in \mathbb{E} \mid j \in \mathcal{N}_i(p^g)\}$. Then, the pair $G(p^g) := (\mathbb{N}, \mathcal{E}(p^g))$ is called the *proximity net* of the group. The proximity net of a group is an undirected graph with nodes $\mathbb{N}$ and edges $\mathcal{E}(p^g)$.
- Denote the union of all proximity nets across a nonempty finite time interval $[t_k, t_l)$ by $\mathcal{G}(t_k, t_l)$, whose edges are the union of the edges of those proximity nets at all the time points over this time interval, that is

$$\mathcal{G}(t_k, t_l) := (\mathbb{N}, \cup_{t\in[t_k,t_l)}\mathcal{E}(p^g(t))).$$

  Then, the group is called *jointly connected* over $[t_k, t_l)$ if and only if $\mathcal{G}(t_k, t_l)$ is connected.

Remark 4: From the definition of neighborhood $\mathcal{N}_i(p^g)$, a nearest neighborhood rule is adopted and it results in a time varying but undirected graph. If the communication radii of the vehicles are different, the proximity net of the group will be a directed graph. For an undirected graph, each pair of

vehicles receives symmetric influences from each other and the average of the quantities for consensus is maintained as a constant. This is the main technique underlying the analysis of the proposed control algorithm. But for a directed (i.e., nonsymmetric) and time-varying graph, this technique is not valid any more. This situation is practically interesting but becomes more challenging.

Definition 5: For any two vehicles i and j of the group (2)

$$\delta_{ij}(t) = \max\{r - \left\|p_{ij}^g(t)\right\|, 0\}, \quad p_{ij}^g(t) := p_i^g(t) - p_j^g(t)$$

and

$$\delta_{ij}(t_k, t_l) = \sup_{t\in[t_k,t_l)} \delta_{ij}(t)$$

are called their *connectivity intensity* at t and over $[t_k, t_l)$, respectively.

Remark 6: Clearly, when $\|p_{ij}^g(t)\| \geq r$, vehicles i and j are not neighbors and their connectivity intensity is $\delta_{ij}(t) = 0$; when $\|p_{ij}^g(t)\| < r$, vehicles i and j are neighbors and their connectivity intensity is $\delta_{ij}(t) > 0$, which becomes larger when the two vehicles get closer. Moreover, $\delta_{ij}(t_k, t_l)$ represents the deepest position vehicle i gets into the neighborhood of j during the time interval $[t_k, t_l)$.

Definition 7: For any two vehicles i and j of the group (2)

$$d_{ij}(t_k, t_l) := \max_{2\leq r\leq n, m_1=i, m_2, \ldots, m_{r-1}, m_r=j\in\mathbb{N}} \times \left\{\min_{s=1,\ldots,r-1} \delta_{m_s,m_{s+1}}(t_k, t_l)\right\}$$

is called their *joint connectivity intensity* over $[t_k, t_l)$. Moreover, the group has a *joint connectivity intensity* $d_o \geq 0$ over $[t_k, t_l)$ if

$$d_{ij}(t_k, t_l) \geq d_o \quad \forall (i, j) \in \mathbb{E}.$$

Remark 8: For a sequence

$$i = m_1, m_2, \ldots, m_{r-1}, \quad m_r = j$$

each pair of adjoining vehicles get into each other's outer neighborhood by the deepness of at least $\min_{s=1,\ldots,r-1} \delta_{m_s m_{s+1}}(t_k, t_l)$, which is the weakest connection between vehicles k and j and hence defines their joint connectivity intensity along the given sequence. Thereby, $d_{ij}(t_k, t_l)$ is the joint connectivity intensity between vehicles i and j along the best sequence with which the intensity is maximized.

III. Main Results

The controller of the form (6) is explicitly proposed in this section with the compensator state $z_i = [q_i^{\mathrm{T}}, \sigma_i, \theta_i]^{\mathrm{T}}$ for $q_i \in \mathbb{R}^2$, $\sigma_i \in \mathbb{R}$, and $\theta_i \in \mathbb{R}$. More specifically, the controller takes the following form:

$$u_i = r_i(\sigma_i, \theta_i, v_i, w_i, \tau_i) - \kappa_i[p_i - s_i(q_i, \sigma_i, \theta_i)], \quad \kappa_i > 0 \tag{7}$$

and

$$\begin{aligned} \dot{q}_i &= v_i \\ \dot{\sigma}_i &= w_i. \end{aligned} \tag{8}$$

The state $\theta_i(t)$, governed by $\dot{\theta}_i = \tau_i$, describes the motion along the curve in time course. For example, it can be simply generated with $\tau_i = 1$. The controller variables v_i and w_i are designed for consensus on the center and on the orientation, respectively. For this purpose, it is assumed that the function $\wp(\theta_i)$ has the following property, in particular, the size is bounded.

Assumption 9: The function $\wp(\theta_i)$ is continuously differentiable and satisfies

$$\|a_i \wp(\theta_i)\| \leq a_0 \quad \forall \theta_i \in \mathbb{R}$$

for a constant a_0.

The controller involves two concurrent actions. First, in the controller, the terms r_i and s_i are designed to regulate vehicle i's trajectory to a desired motion pattern specified by the center q_i and orientation σ_i. Specifically, they are defined as follows, respectively:

$$\begin{aligned} r_i(\sigma_i, \theta_i, v_i, w_i, \tau_i) = v_i &+ a_i \wp'(\theta_i)\tau_i \begin{bmatrix} \cos(\theta_i + \sigma_i) \\ \sin(\theta_i + \sigma_i) \end{bmatrix} \\ &+ a_i \wp(\theta_i) \begin{bmatrix} -\sin(\theta_i + \sigma_i)(\tau_i + w_i) \\ \cos(\theta_i + \sigma_i)(\tau_i + w_i) \end{bmatrix} \end{aligned}$$

and

$$s_i(q_i, \sigma_i, \theta_i) = q_i + a_i \wp(\theta_i) \begin{bmatrix} \cos(\theta_i + \sigma_i) \\ \sin(\theta_i + \sigma_i) \end{bmatrix}.$$

Also, the control variables v_i and w_i are designed in a decentralized manner to achieve consensus of motion centers q_i and orientations σ_i of all vehicles for $i = 1, \ldots, n$. Specifically, they are calculated as follows:

$$\begin{aligned} v_i &= \sum_{j\in\mathcal{N}_i} -a_v(\|\ell_{ij}\|)[q_i - p_i - S(-\ell_{ji}, \ell_{ij})(q_j - p_j) + \ell_{ij}] \\ w_i &= \sum_{j\in\mathcal{N}_i} -a_w(\|\ell_{ij}\|)[\sigma_i - \sigma_j - \varrho(-\ell_{ji}, \ell_{ij})]. \end{aligned}$$

The functions $a_v(\cdot)$ and $a_w(\cdot)$ are Lipschitz continuous. Moreover, they are positive if and only if they are at the interval $[0, r)$, denoted by $a_v, a_w \in \mathcal{S}$ for

$$\mathcal{S} = \{f : [0, \infty) \mapsto \mathbb{R} | f(x) = 0 \quad \forall x \geq r;\ f(x) > 0 \quad \forall x < r\}.$$

The functions $S : (\mathbb{R}^2 \times \mathbb{R}^2) \mapsto \mathbb{R}^{2\times 2}$ and $\varrho : (\mathbb{R}^2 \times \mathbb{R}^2) \mapsto \mathbb{R}$ are defined as follows, for $x = [x_1, x_2]^{\mathrm{T}}$ and $y = [y_1, y_2]^{\mathrm{T}}$:

$$\begin{aligned} S(x, y) &= \frac{1}{\|x\|\|y\|} \begin{bmatrix} x_1 & x_2 \\ -x_2 & x_1 \end{bmatrix} \begin{bmatrix} y_1 & -y_2 \\ y_2 & y_1 \end{bmatrix} \\ \varrho(x, y) &= \arccos\left(\frac{x^{\mathrm{T}}y}{\|x\|\|y\|}\right). \end{aligned}$$

It is easy to check

$$S(x, y)S^{\mathrm{T}}(x, y) = I_2, \quad \det[S(x, y)] = 1$$

that is, $S(x, y)$ is a rotation matrix. Also, direct calculation shows $y/\|y\| = S(x, y)x/|x\|$, and hence $y = S(x, y)x$ if $\|x\| = \|y\|$.

Next, suppose the network satisfies a joint connectivity condition given below. Various joint connectivity conditions have been widely used for collective behavior analysis in [20] and [27]–[29].

Assumption 10: The group of vehicles is uniformly jointly connected, in particular, there exists an infinite time sequence $t_1 < t_2 < t_3 < \cdots$, with $t_\infty = \infty$, such that the group (2) has a joint connectivity intensity $d_o > 0$ over every bounded time interval $[t_k, t_{k+1}),\ k = 1, 2, \ldots$.

Now, we are ready to have the main result.

Theorem 11: The group of vehicles (2) with the dynamic controller (7), (8) achieves the collective motion of the pattern $\wp(\theta)$ under Assumptions 9 and 10 if $r > 2a_0$.

Proof: We divide the proof into three steps.

Step 1: Define a variable

$$\bar{p}_i = s_i(q_i, \sigma_i, \theta_i) = q_i + a_i \wp(\theta_i) \begin{bmatrix} \cos(\theta_i + \sigma_i) \\ \sin(\theta_i + \sigma_i) \end{bmatrix}.$$

Simple calculation shows

$$\begin{aligned} \dot{\bar{p}}_i = \dot{q}_i + a_i \wp'(\theta_i)\dot{\theta}_i \begin{bmatrix} \cos(\theta_i + \sigma_i) \\ \sin(\theta_i + \sigma_i) \end{bmatrix} \\ + a_i \wp(\theta_i) \begin{bmatrix} -\sin(\theta_i + \sigma_i)(\dot{\theta}_i + \dot{\sigma}_i) \\ -\cos(\theta_i + \sigma_i)(\dot{\theta}_i + \dot{\sigma}_i) \end{bmatrix} \end{aligned}$$

and hence

$$\begin{aligned} \dot{\bar{p}}_i = v_i + a_i \wp'(\theta_i)\tau_i \begin{bmatrix} \cos(\theta_i + \sigma_i) \\ \sin(\theta_i + \sigma_i) \end{bmatrix} \\ + a_i \wp(\theta_i) \begin{bmatrix} -\sin(\theta_i + \sigma_i)(\tau_i + w_i) \\ \cos(\theta_i + \sigma_i)(\tau_i + w_i) \end{bmatrix} = r_i(\sigma_i, \theta_i, v_i, w_i, \tau_i). \end{aligned}$$

Let $e_i = p_i - \bar{p}_i$ be the difference between p_i and $\bar{p}_i$. With the controller

$$\dot{e}_i = u_i - r_i(\sigma_i, \theta_i, v_i, w_i, \tau_i) = -\kappa_i e_i.$$

As a result

$$\lim_{t\to\infty} p_i(t) - \bar{p}_i(t) = 0$$

and hence

$$\lim_{t\to\infty} p_i^g(t) - \bar{p}_i^g(t) = 0 \tag{9}$$

for $\bar{p}_i^g = R_i \bar{p}_i + \xi_i$.

Step 2: Define two variables

$$q_i^g = R_i q_i + \xi_i, \quad \sigma_i^g = \sigma_i + \rho_i.$$

Simple calculation shows

$$\dot{q}_i^g = R_i v_i, \quad \dot{\sigma}_i^g = w_i.$$

On the one hand, by noting $R_i \ell_{ij} = -R_j \ell_{ji}$, i.e., $\ell_{ij} = -R_i^{-1} R_j \ell_{ji}$ and $\|\ell_{ij}\| = \|-\ell_{ji}\|$, the rotation matrix $R_i^{-1} R_j$ can be calculated as follows:

$$R_i^{-1} R_j = S(-\ell_{ji}, \ell_{ij}).$$

Further calculation shows

$$\begin{aligned} R_i^{-1}\big(q_i^g - q_j^g\big) &= R_i^{-1}\big(q_i^g - p_i^g - q_j^g + p_j^g\big) + R_i^{-1}\big(p_i^g - p_j^g\big) \\ &= q_i - p_i - R_i^{-1} R_j (q_j - p_j) + \ell_{ij} \\ &= q_i - p_i - S(-\ell_{ji}, \ell_{ij})(q_j - p_j) + \ell_{ij}. \end{aligned}$$

As a result

$$v_i = \sum_{j\in\mathcal{N}_i} -a_v(\|\ell_{ij}\|) R_i^{-1}\big(q_i^g - q_j^g\big).$$

On the other hand, we note that the $(1, 1)$ entry of $R_i^{-1} R_j$ is $\cos(\rho_j - \rho_i)$. That is

$$\cos(\rho_j - \rho_i) = S_{11}(-\ell_{ji}, \ell_{ij})$$

or

$$\rho_j - \rho_i = \arccos(S_{11}(-\ell_{ji}, \ell_{ij})) = \varrho(-\ell_{ji}, \ell_{ij}).$$

Further calculation shows

$$\sigma_i^g - \sigma_j^g = \sigma_i + \rho_i - \sigma_j - \rho_j = \sigma_i - \sigma_j - \varrho(-\ell_{ji}, \ell_{ij}).$$

Then

$$w_i = \sum_{j\in\mathcal{N}_i} -a_w(\|\ell_{ij}\|)\big(\sigma_i^g - \sigma_j^g\big).$$

From the above development, one has

$$\dot{q}_i^g = -\sum_{j\in\mathcal{N}_i} a_v(\|\ell_{ij}\|)\big(q_i^g - q_j^g\big) \tag{10}$$

$$\dot{\sigma}_i^g = -\sum_{j\in\mathcal{N}_i} a_w(\|\ell_{ij}\|)\big(\sigma_i^g - \sigma_j^g\big). \tag{11}$$

As a result, we can prove that

$$\lim_{t\to\infty} q_i^g(t) - q^o = 0, \quad \lim_{t\to\infty} \sigma_i^g(t) - \sigma^o = 0, \quad i = 1, \ldots, n \tag{12}$$

for some constants q^o and σ^o. The details are given below.

Let $\tilde{q}(t) := \sum_{i\in\mathbb{N}} q_i^g(t)/n$. Direct calculation shows that

$$d\tilde{q}(t)/dt = -(1/n) \sum_{(i,j)\in\mathbb{E}} a_v(\|\ell_{ij}\|) q_{ij}^g/2 = 0 \tag{13}$$

due to $a_v(\|\ell_{ij}\|) = a_v(\|\ell_{ji}\|)$ and $q_{ij}^g = -q_{ji}^g$. In other words, $\tilde{q}(t)$ is a constant and we denote this constant by q^o, i.e., $q^o = \tilde{q}(t), \forall t \geq 0$.

Let us define an energy function

$$V(q^g) = \frac{1}{2} \sum_{i\in\mathbb{N}} \big\|q_i^g - q^o\big\|^2. \tag{14}$$

Obviously, the energy function is nonnegative and it reduces to zero if and only if $q_i^g = q^o$ for all $i \in \mathbb{N}$. Next, we will show that the energy function $V(q^g)$ does not increase along the trajectory of system (10). To this end, we note that

$$\begin{aligned} \frac{dV(q^g)}{dt} &= \frac{\partial V(q^g)}{\partial q^g} \dot{q}^g \\ &= -\sum_{(i,j)\in\mathbb{E}} a_v(\|\ell_{ij}\|)\big(q_i^g - q^o\big)^{\mathsf{T}}\big(q_i^g - q_j^g\big) \\ &= -\sum_{(i,j)\in\mathbb{E}} a_v(\|\ell_{ij}\|)\big(q_i^g\big)^{\mathsf{T}}\big(q_i^g - q_j^g\big) \\ &= -\sum_{(i,j)\in\mathbb{E}} a_v(\|\ell_{ij}\|)\big\|q_{ij}^g\big\|^2/2 \leq 0. \end{aligned} \tag{15}$$

By LaSalle's invariance principle, we have

$$\lim_{t\to\infty} dV(q^g(t))/dt = 0.$$

More specifically, we denote $s(t) := V(q^g(t))$ and hence

$$\dot{s}(t) = -\sum_{(i,j)\in\mathbb{E}} a_v(\|\ell_{ij}(t)\|)\big\|q_{ij}^g(t)\big\|^2/2 \leq 0.$$

Property (15) implies that $q^g(t)$ is bounded. Moreover, direct calculation shows that $\dot{\ell}_{ij}(t)$ and $\dot{q}^g_{ij}(t)$ are bounded, that is, $\ell_{ij}(t)$ and $q^g_{ij}(t)$ are uniformly continuous in t. As $a_v(\cdot)$ is Lipschitz continuous, the function $\dot{s}(t)$ is also uniformly continuous in t. Obviously, $s(t)$ is a continuously differentiable function in t. For $\dot{s}(t) \leq 0$ and $s(t) \geq 0$, $s(t)$ has a finite limit as $t \to \infty$. Therefore, by Barbalat's Lemma, we obtain $\lim_{t\to\infty} \dot{s}(t) = 0$, i.e., $\lim_{t\to\infty} dV(q^g(t))/dt = 0$. Equivalently, we have

$$\lim_{t\to\infty} a_v(\|\ell_{ij}(t)\|)\left\|q^g_{ij}(t)\right\|^2 = 0 \quad \forall (i,j) \in \mathbb{E}. \tag{16}$$

In the previous step, we have shown (9). Therefore, for any $\varrho > 0$, there exists a positive time T_1, such that

$$\left\| p^g_i(t) - \bar{p}^g_i(t) \right\| < \varrho/2 \quad \forall t \geq T_1. \tag{17}$$

Detailed calculation shows

$$\begin{aligned}\bar{p}^g_i &= R_i \bar{p}_i + \xi_i = R_i q_i + R_i a_i \wp(\theta_i) \begin{bmatrix} \cos(\theta_i + \sigma_i) \\ \sin(\theta_i + \sigma_i) \end{bmatrix} + \xi_i \\ &= q^g_i + a_i \wp(\theta_i) \begin{bmatrix} \cos(\theta_i + \sigma^g_i) \\ \sin(\theta_i + \sigma^g_i) \end{bmatrix}.\end{aligned}$$

When $q^g_{ij} = q^g_i - q^g_j = 0$, one has, using Assumption 9

$$\|\bar{p}^g_i(t) - \bar{p}^g_j(t)\| \leq \|a_i \wp(\theta_i(t))\| + \|a_j \wp(\theta_j(t))\| \leq 2a_0. \tag{18}$$

Combining (17) and (18) gives, for $t \geq T_1$

$$\left\| p^g_i(t) - p^g_j(t) \right\| \leq 2a_0 + \varrho$$

and hence

$$\|\ell_{ij}(t)\| \leq 2a_0 + \varrho.$$

Under the condition $r > 2a_0$. Let $\lambda = r - 2a_0 > 0$ and $\varrho = \lambda/2$

$$\|\ell_{ij}(t)\| \leq r - \lambda/2.$$

As a result

$$\alpha_v(\|\ell_{ij}(t)\|) \geq \gamma \tag{19}$$

for $\gamma = \min_{x\in[0, r-\lambda/2]} \alpha_v(x) > 0$. Hence, there exists a positive number $l > 0$, independent of t, such that

$$\alpha_v(\|\ell_{ij}(t)\|) \geq \gamma/2 \quad \forall \|q^g_{ij}\| < l \quad \forall t \geq T_1.$$

Next, we pick an arbitrary real number $0 < \epsilon < l/n$. Denote

$$\mathbb{I}_1 := [\epsilon,\ l - \epsilon] \subset \mathbb{I}_2 := [\epsilon/2,\ l - \epsilon/2].$$

From (16), there exists a finite time $T_2 \geq T_1$, such that

$$\alpha_v(\|\ell_{ij}(t)\|)\left\|q^g_{ij}(t)\right\|^2 < \alpha_v(r - d_o)(l - \epsilon)^2 \quad \forall t \geq T_2 \tag{20}$$

where d_o is the joint connectivity intensity in Assumption 10.

In what follows, we will prove two claims.

Claim 12: There exist a time $T_3 \geq T_2$ such that $\|q^g_{ij}(t)\| \notin \mathbb{I}_1$, $\forall t \geq T_3$, $\forall (i,j) \in \mathbb{E}$.

For a time t^*, if $\|q^g_{ij}(t^*)\| \in \mathbb{I}_1$, then we have $\|q^g_{ij}(\tau)\| \in \mathbb{I}_2$ and hence $\epsilon/2 \leq \|q^g_{ij}(\tau)\| \leq l - \epsilon/2$, for $\tau \in [t^*, t^* + \bar{t}]$ because it takes a time longer than some $\bar{t}$ to move from inside of $\mathbb{I}_1$ to outside of $\mathbb{I}_2$ [noting that $q^g_{ij}(t)$ is continuous in t]. As a result

$$\alpha_v(\|\ell_{ij}(\tau)\|) \geq \gamma/2$$

and hence

$$\alpha_v(\|\ell_{ij}(\tau)\|)\left\|q^g_{ij}(\tau)\right\|^2 > \epsilon^2\gamma/8.$$

If the claim is not true, t^* and hence τ can be arbitrarily large, which contradicts (16).

Claim 13: For the time T_3 given in Claim 12, $\|q^g_{ij}(t)\| < \epsilon$, $\forall t \geq T_3$, $\forall (i,j) \in \mathbb{E}$.

If the claim it not true, there exists a pair $(\hbar, \ell) \in \mathbb{E}$ such that $\|q^g_{\hbar\ell}(t)\| \geq \epsilon$ for some time $t \geq T_3$. However, due to Claim 12, $\|q^g_{\hbar\ell}(t)\| \notin \mathbb{I}_1$, $\forall t \geq T_3$. Therefore, $\|q^g_{\hbar\ell}(t)\| > l - \epsilon$, $\forall t \geq T_3$. Under Assumption 10, there exists a sequence $\hbar = m_1, m_2, \ldots, m_{h-1}, m_h = \ell$, (without loss of generality, we assume $m_i = i$ to save the notations) such that

$$\alpha_v(\|\ell_{i(i+1)}(\tau_i)\|) \geq \alpha_v(r - d_o), \quad i = 1, \ldots, h-1 \tag{21}$$

for some $\tau_i \geq T_3$. On the other hand, there exists $1 \leq \kappa < h$ such that

$$\left\|q^g_{\kappa(\kappa+1)}(t)\right\| > l - \epsilon \quad \forall t \geq T_3. \tag{22}$$

Otherwise, using Claim 12 again, we have

$$\left\|q^g_{i(i+1)}(t)\right\| < \epsilon \quad \forall t \geq T_3, \quad i = 1, \ldots, h-1$$

and hence

$$\left\|q^g_{\hbar\ell}(t)\right\| \leq \sum_{i=1}^{h-1} \left\|q^g_{i(i+1)}(t)\right\| < (N-1)\epsilon < l - \epsilon \quad \forall t \geq T_3$$

which contradicts that $\|q^g_{\hbar\ell}(t)\| > l - \epsilon$, $\forall t \geq T_3$. From (21) and (22), at the moment τ_κ, we have

$$\alpha_v(\|\ell_{\kappa(\kappa+1)}(\tau_\kappa)\|)\left\|q^g_{\kappa(\kappa+1)}(\tau_\kappa)\right\|^2 > \alpha_v(r - d_o)(l - \epsilon)^2$$

which contradicts (20), and Claim 13 is thus proved.

From Claim 13, since ϵ can be arbitrarily small, we have

$$\lim_{t\to\infty} \left\|q^g_{ij}(t)\right\| = 0 \quad \forall (i,j) \in \mathbb{E}$$

that is

$$\lim_{t\to\infty} q^g_i(t) - q^o = 0. \tag{23}$$

For the same argument, one has $\lim_{t\to\infty} \sigma^g_i(t) - \sigma^o = 0$ for some constant σ^o. The proof of (12) is complete.

Step 3: Finally, let

$$p^o_i(t) := q^o + a_i \wp(\theta_i(t)) \angle(\theta_i(t) + \sigma^o), \quad i = 1, \ldots, n.$$

Note

$$\bar{p}^g_i(t) = q^g_i(t) + a_i \wp(\theta_i(t)) \angle(\theta_i(t) + \sigma^g_i(t)).$$

Therefore, $\lim_{t\to\infty} \bar{p}^g_i(t) - p^o_i(t) = 0$ which, together with (9), implies $\lim_{t\to\infty} p^g_i(t) - p^o_i(t) = 0$, i.e., (4). The proof is thus complete.

Remark 14: It can be seen from Theorem 11 that the collective behavior mainly consists of two actions. First, using a feedforward controller, each agent achieves the regulation between its output of first-order dynamics and the reference

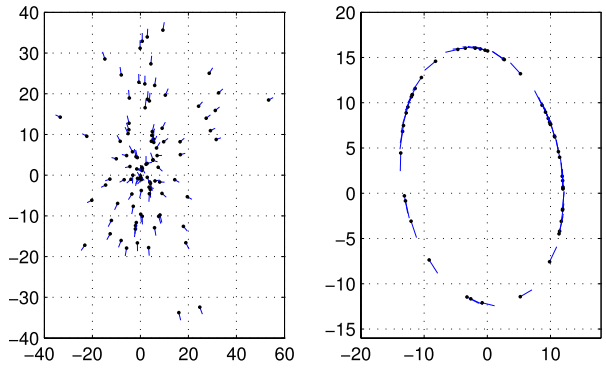

Fig. 1. Output synchronization in an elliptical pattern. Left: the initial distribution of 50 vehicles ($t = 0$ s). Right: the pattern synchronization occurs ($t = 4$ s). The dots represent the vehicles' positions and the short lines represent their velocities.

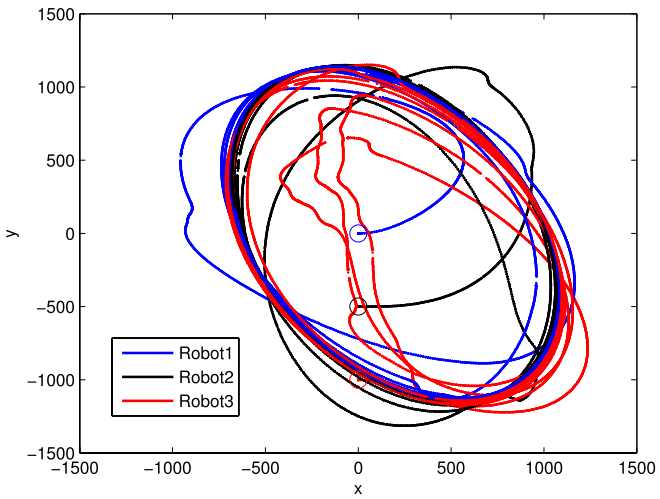

Fig. 2. Trajectories of three robots. The initial positions are marked as ○.

trajectory in the sense of (17). In fact, the regulation problem can be similarly solved for more complicated systems, e.g., second-order dynamics. Second, with a properly designed algorithm, the reference models achieve consensus in the sense of (23). This action is independent of agent dynamics. Overall, the approach studied in this brief is also applicable for agents of more complicated dynamics.

IV. Numerical Simulation and Experiments

Consider a group of vehicles moving in 2-D space. They aim to achieve synchronization in an elliptical pattern (3) with $a = 15$ and $b = 12$. The simulation result based on the decentralized controller proposed in this brief, with $n = 50$, is shown in Fig. 1. The initial distribution of the agents is plotted in the left graph. In 4 s, the group of agents achieves synchronization in an elliptical pattern as shown in the right graph.

An experimental multirobot system is used to examine the practical applicability of the control algorithm proposed in this brief. The multirobot system is composed of three Amigobot robots of Adept MobileRobots. The detailed description of the experimental platform in hardware and software can be found in [30]. Specifically, the actuating signals of an Amigobot are its linear and angular velocities, i.e., $\mathrm{u}_i^l \in \mathbb{R}$ and $\mathrm{u}_i^a \in \mathbb{R}$. Let $\xi_i \in \mathbb{R}^2$ be the center of the Amigobot and ϕ_i the angle of its moving direction relative to the positive x-axis of Σ_i. Then, Amigobots have the following kinematic model:

$$\dot{\xi}_i(t) = \begin{bmatrix} \cos\phi_i(t) \\ \sin\phi_i(t) \end{bmatrix} \mathrm{u}_i^l(t), \quad \dot{\phi}_i(t) = \mathrm{u}_i^a(t). \tag{24}$$

A new coordinate

$$p_i = \xi_i + d \begin{bmatrix} \cos\phi_i \\ \sin\phi_i \end{bmatrix}$$

is introduced to simplify model (24) to (2)

$$\dot{p}_i = \dot{\xi}_i + d \begin{bmatrix} -\sin\phi_i \\ \cos\phi_i \end{bmatrix} \dot{\phi}_i = u_i \tag{25}$$

under the controller

$$\begin{bmatrix} \mathrm{u}_i^l \\ \mathrm{u}_i^a \end{bmatrix} = \begin{bmatrix} \cos\phi_i & \sin\phi_i \\ -(1/d)\sin\phi_i & (1/d)\cos\phi_i \end{bmatrix} u_i \tag{26}$$

where u_i is designed in (7). The parameter $d > 0$ can be selected to have a practically reasonable angular velocity ω_i. In particular, it can be chosen as the radius of robot.

In practical controller implementation for robots of significant size, a collision avoidance algorithm must be considered. Once the sonar array of a robot detects another robot in its front sector ring characterized by radius and angle range, the robot switches to a collision avoidance mode. A more detailed explanation of the collision avoidance algorithm used in this brief can be found in [31]. Specifically, the robot slows down and deviates to avoid collision until there is no object in the front sector. Afterward, it switches back to the proposed pattern motion controller. When the robots are close to form the desired motion pattern after a few times of collision avoidance, they are usually sufficiently separated and the collision avoidance algorithm will not take affect any longer. As a result, the desired motion can be guaranteed. We consider collision avoidance as a practical issue in real implementation. But it is challenging to theoretically prove the stability for the proposed pattern motion controller integrated with the collision avoidance algorithm.

In the experiments, the complete moving trajectories of all robots were recorded in an odometer log and plotted in Fig. 2. It was observed that all the three robots initially moved along their own trajectories, and the motion trajectories eventually converged to an ellipse with a common center and a common orientation after several times of interactions. To demonstrate the convergence procedure of the motion centers and orientations of all robots more clearly, we define

$$q_e^g(t) = \frac{1}{2}\sum_{i\neq j} \left\| q_i^g(t) - q_j^g(t) \right\|$$

$$\sigma_e^g(t) = \frac{1}{2}\sum_{i\neq j} \left\| \sigma_i^g(t) - \sigma_j^g(t) \right\|.$$

Once the consensus in an elliptical pattern is achieved, one has $\lim_{t\to\infty} q_e^g(t) = 0$ and $\lim_{t\to\infty} \sigma_e^g(t) = 0$. This convergence profile is illustrated in Fig. 3. In more detail, it was observed as expected that $q_e^g(t)$ and $\sigma_e^g(t)$ approach zero in about 5 min.

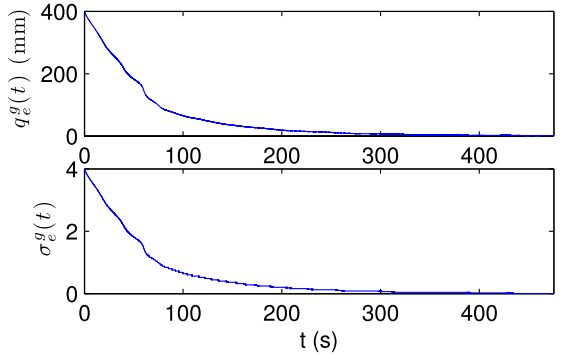

Fig. 3. Convergence performance of the motion centers and orientations.

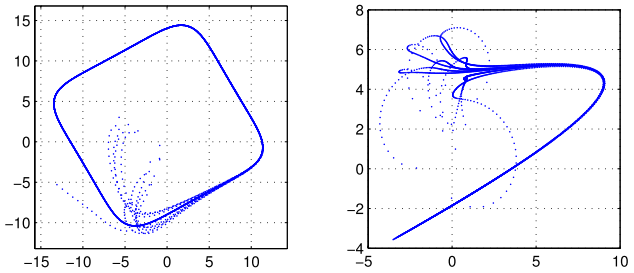

Fig. 4. Trajectories of ten robots achieving collective motion of smoothened square and parabolic patterns.

Finally, the control algorithm proposed in this brief is also examined for smoothened square and parabolic patterns with

$$\wp(\theta) = \frac{10}{\sqrt[6]{(\cos\theta)^6 + (\sin\theta)^6}}$$

$$\wp(\theta) = \frac{\sin\theta + \sqrt{(\sin\theta)^2 + 40(\cos\theta)^2}}{2(\cos\theta)^2}.$$

For the open parabolic path, we consider a specified segment between two points whose size is finite and satisfies Assumption 9. The complete trajectories are shown in Fig. 4.

V. Conclusion

In this brief, a completely decentralized control algorithm has been proposed for a group of autonomous multivehicles to form a class of collective behavior in diverse motion patterns. The approach has been demonstrated by simulation and experiments with guaranteed convergence of motion centers and orientations.

References

[1] S. Martinez, J. Cortes, and F. Bullo, "Motion coordination with distributed information," *IEEE Control Syst. Mag.*, vol. 27, no. 4, pp. 75–88, Aug. 2007.

[2] H.-T. Zhang, N. Wang, R.-Q. Su, M. Z. Q. Chen, T. Zhou, and C. Zhou, "Spatially quantifying the leadership effectiveness in collective behavior," *New J. Phys.*, vol. 12, p. 12305, Dec. 2010.

[3] Z. Cheng, H.-T. Zhang, M. Z. Q. Chen, T. Zhou, and N. V. Valeyev, "Aggregation pattern transitions by slightly varying the attractive/repulsive function," *PLoS ONE*, vol. 6, no. 7, p. e22123, 2011.

[4] J. Halloy *et al.*, "Social integration of robots into groups of cockroaches to control self-organized choices," *Science*, vol. 318, no. 5853, pp. 1155–1158, 2007.

[5] J. Buhl *et al.*, "From disorder to order in marching locusts," *Science*, vol. 312, no. 5778, pp. 1402–1406, Jun. 2006.

[6] N. E. Leonard and E. Fiorelli, "Virtual leaders, artificial potentials and coordinated control of groups," in *Proc. 40th IEEE Conf. Decision Control*, Dec. 2001, pp. 2968–2973.

[7] E. W. Justh and P. S. Krishnaprasad, "Equilibria and steering laws for planar formations," *Syst. Control Lett.*, vol. 52, no. 1, pp. 25–38, May 2004.

[8] D. Paley, N. E. Leonard, and R. Sepulchre, "Collective motion: Bistability and trajectory tracking," in *Proc. 43rd IEEE Conf. Decision Control*, Dec. 2004, pp. 1932–1937.

[9] J. A. Marshall, M. E. Broucke, and B. A. Francis, "Formations of vehicles in cyclic pursuit," *IEEE Trans. Autom. Control*, vol. 49, no. 11, pp. 1963–1974, Nov. 2004.

[10] J. Jeanne, N. E. Leonard, and D. Paley, "Collective motion of ring-coupled planar particles," in *Proc. 44th IEEE Conf. Decision Control*, Dec. 2005, pp. 3929–3934.

[11] M. Pavone and E. Frazzoli, "Decentralized policies for geometric pattern formation and path coverage," *ASME J. Dyn. Syst., Meas., Control*, vol. 129, no. 5, pp. 633–643, 2007.

[12] W. Ren, "Collective motion from consensus with Cartesian coordinate coupling," *IEEE Trans. Autom. Control*, vol. 54, no. 6, pp. 1330–1335, Jun. 2009.

[13] P. Lin and Y. Jia, "Distributed rotating formation control of multi-agent systems," *Syst. Control Lett.*, vol. 59, no. 10, pp. 587–595, Oct. 2010.

[14] P. Lin, K. Qin, Z. Li, and W. Ren, "Collective rotating motions of second-order multi-agent systems in three-dimensional space," *Syst. Control Lett.*, vol. 60, no. 6, pp. 365–372, Jun. 2011.

[15] R. Sepulchre, D. A. Paley, and N. E. Leonard, "Stabilization of planar collective motion with limited communication," *IEEE Trans. Autom. Control*, vol. 53, no. 3, pp. 706–719, Apr. 2008.

[16] L. Scardovi, N. Leonard, and R. Sepulchre, "Stabilization of three-dimensional collective motion," *Commun. Inf. Syst.*, vol. 8, no. 4, pp. 473–500, 2008.

[17] A. Sarlette and R. Sepulchre, "Consensus optimization on manifolds," *SIAM J. Control Optim.*, vol. 48, no. 1, pp. 56–76, 2009.

[18] N. Ceccarelli, M. D. Marco, A. Garulli, and A. Giannitrapani, "Collective circular motion of multi-vehicle systems," *Automatica*, vol. 44, no. 12, pp. 3025–3035, Dec. 2008.

[19] Z. Chen and H.-T. Zhang, "No-beacon collective circular motion of jointly connected multi-agents," *Automatica*, vol. 47, no. 9, pp. 1929–1937, Sep. 2011.

[20] Z. Chen and H.-T. Zhang, "A remark on collective circular motion of heterogeneous multi-agents," *Automatica*, vol. 49, no. 5, pp. 1236–1241, May 2013.

[21] P. Wieland, R. Sepulchre, and F. Allgöwer, "An internal model principle is necessary and sufficient for linear output synchronization," *Automatica*, vol. 47, no. 5, pp. 1068–1074, May 2011.

[22] H. Kim, H. Shim, and J. H. Seo, "Output consensus of heterogeneous uncertain linear multi-agent systems," *IEEE Trans. Autom. Control*, vol. 56, no. 1, pp. 200–206, Jan. 2011.

[23] Z. Chen, "Pattern synchronization of nonlinear heterogeneous multiagent networks with jointly connected topologies," *IEEE Trans. Control Netw. Syst.*, vol. 1, no. 4, pp. 349–359, Dec. 2014.

[24] A. Isidori, L. Marconi, and G. Casadei, "Robust output synchronization of a network of heterogeneous nonlinear agents via nonlinear regulation theory," *IEEE Trans. Autom. Control*, vol. 59, no. 10, pp. 2680–2691, Oct. 2014.

[25] X. Chen and Z. Chen, "Robust perturbed output regulation and synchronization of nonlinear heterogeneous multi-agents," *IEEE Trans. Cybern.*, to be published.

[26] L. Zhu, Z. Chen, and R. Middleton, "A general framework for robust output synchronization of heterogeneous nonlinear networked systems," *IEEE Trans. Autom. Control*, DOI 10.1109/TAC.2015.2492141

[27] H.-T. Zhang, C. Zhai, and Z. Chen, "A general alignment repulsion algorithm for flocking of multi-agent systems," *IEEE Trans. Autom. Control*, vol. 56, no. 2, pp. 430–435, Feb. 2011.

[28] R. Olfati-Saber and R. M. Murray, "Consensus problems in networks of agents with switching topology and time-delays," *IEEE Trans. Autom. Control*, vol. 49, no. 9, pp. 1520–1533, Sep. 2004.

[29] Y. Hong, L. Gao, D. Cheng, and J. Hu, "Lyapunov-based approach to multiagent systems with switching jointly connected interconnection," *IEEE Trans. Autom. Control*, vol. 52, no. 5, pp. 943–948, May 2007.

[30] Z. Chen, H.-T. Zhang, M.-C. Fan, D. Wang, and D. Li, "Algorithms and experiments on flocking of multiagents in a bounded space," *IEEE Trans. Control Syst. Technol.*, vol. 22, no. 4, pp. 1544–1549, Jul. 2014.

[31] H.-T. Zhang, Z. Chen, L. Yan, and W. Yu, "Applications of collective circular motion control to multirobot systems," *IEEE Trans. Control Syst. Technol.*, vol. 21, no. 4, pp. 1416–1422, Jul. 2013.